INFECTION AND IMMUNITY, Nov. 2008, p. 4978–4988 Vol. 76, No. 11
0019-9567/08/$08.00+0 doi:10.1128/IAI.00736-08

The p50 Subunit of NF-κB Is Critical for In Vivo Clearance of the Noninvasive Enteric Pathogen *Citrobacter rodentium*▽

Alison Dennis,[1] Takahiro Kudo,[1] Laurens Kruidenier,[2] Francis Girard,[3] Valerie F. Crepin,[3] Thomas T. MacDonald,[1] Gad Frankel,[3] and Siouxsie Wiles[3]*

Centre for Infectious Disease, Institute of Cell and Molecular Science, Barts and the London School of Medicine and Dentistry, 4 Newark Street London E1 2AT, United Kingdom[1]; Immuno-Inflammation CEDD, GSK Medicines Research Centre, Gunnels Wood Road, Stevenage, Hertfordshire SG1 2NY, United Kingdom[2]; and Division of Cell and Molecular Biology, Imperial College London, Flowers Building, Exhibition Road, London SW7 2AZ, United Kingdom[3]

Received 10 June 2008/Returned for modification 24 July 2008/Accepted 1 August 2008

***Citrobacter rodentium*, a natural mouse pathogen, belongs to the family of extracellular enteric pathogens that includes enteropathogenic *Escherichia coli* (EPEC) and enterohemorrhagic *E. coli* (EHEC). *C. rodentium* shares many virulence factors with EPEC and EHEC and relies on attaching-and-effacing lesion formation for colonization and infection of the gut. In vivo, *C. rodentium* infection is characterized by increased epithelial cell proliferation, mucosal thickening, and a TH1-type immune response, but with protective immunity believed to be mediated by serum immunoglobulin G (IgG). In this work, we characterize the immune response and pathology of mice lacking the p50 subunit of the transcription factor nuclear factor kappa B (NF-κB) during *C. rodentium* infection. We show that p50$^{-/-}$ mice are unable to clear *C. rodentium* infection. Furthermore, these animals show a reduced influx of immune cells into infected colonic tissue and greater levels of mucosal hyperplasia and the cytokines tumor necrosis factor alpha and gamma interferon. Surprisingly, despite being unable to eliminate infection, p50$^{-/-}$ mice showed markedly higher levels of anti-*Citrobacter* IgG and IgM, suggesting that antibody alone is not responsible for bacterial clearance. These data also demonstrate that non-NF-κB-dependent defenses are insufficient to control *C. rodentium* infection, and hence, the NF-κB p50 subunit is critical for defense against this noninvasive pathogen.**

Enteropathogenic *Escherichia coli* (EPEC) and enterohemorrhagic *E. coli* (EHEC) are highly adapted enteropathogens that successfully colonize the host's gastrointestinal tract via the formation of attaching-and-effacing (A/E) lesions (13). EPEC is a major cause of infantile diarrhea in the developing world, whereas EHEC is a food-borne pathogen in developed countries responsible for bloody diarrhea and hemolytic uremic syndrome due to the action of Shiga toxin (13). EPEC and EHEC exhibit narrow host specificity, and mice are by and large resistant to infection (21). The lack of a simple small-animal model to simulate an in vivo situation makes it difficult to study EPEC and EHEC pathogenesis. In contrast, *Citrobacter rodentium* is a natural mouse pathogen that shares many virulence factors with EPEC and EHEC and relies on A/E lesion formation for colonization and infection of the murine gastrointestinal mucosa (22). As a result, *C. rodentium* has become a popular surrogate model for in vivo studies, providing the ability to manipulate both the pathogen (7) and the host (27), and interesting insights have been gained into the in vivo roles of many gene products that are common to *C. rodentium*, EPEC, and EHEC. In particular, the translocated type III secretion system effector proteins *map*, *espF*, and *tir* have recently been implicated in diarrhea using the *C. rodentium* mouse model (8, 18, 28).

C. rodentium shows a remarkable ability to colonize the murine colon, with over 10^9 bacteria present during the peak of infection. However, by day 21 post-oral challenge, *C. rodentium* is cleared from the gastrointestinal tracts of normal mice (31). Studies have shown that both innate and adaptive immune responses are required for immunity (5, 6, 15, 19, 27), with CD4 T-cell-dependent antibody responses believed to be central to clearance (5). Infection of mice with *C. rodentium* elicits a mucosal TH1 immune response (12) very similar to mouse models of inflammatory bowel disease. Nuclear factor kappa B (NF-κB) is of critical importance in the activation and regulation of the immune response (16). It is ubiquitously expressed in most cell types and regulates a variety of genes responsible for immune function and inflammation (23, 26). NF-κB is considered crucial in maintaining intestinal inflammation during host defense (23), and a high level of activation is thought to be a causative factor in the development of colitis and chronic inflammatory bowel disease (20, 24). Thus, NF-κB has become a potential therapeutic target in the control of chronic intestinal inflammation.

NF-κB is a transcription factor composed of homodimers and heterodimers of Rel proteins, of which there are five members in mammalian cells (NF-κB1 [p50], NF-κB2 [p52], RelA [p65], c-Rel, and RelB) (16). While NF-κB is most commonly a heterodimer composed of p50 and p65 subunits, the various hetero- and homodimers of NF-κB have different tissue expression patterns, binding specificities, and interactions, indicating discrete functions in the immune response (17). NF-κB dimers are held in the cytoplasm in an inactive state by inhibitory proteins known as IκBs. NF-κB activation entails the signal-induced phosphorylation and degradation of IκB molecules, which in turn releases NF-κB to translocate into the

* Corresponding author. Present address: Department of Infectious Diseases and Immunity, Imperial College London, Commonwealth Building 8N12, Du Cane Road, London W12 0NN, United Kingdom. Phone: 44 (0)20 8383 2730. Fax: 44 (0)20 8383 3394. E-mail: siouxsie.wiles@imperial.ac.uk.

▽ Published ahead of print on 11 August 2008.

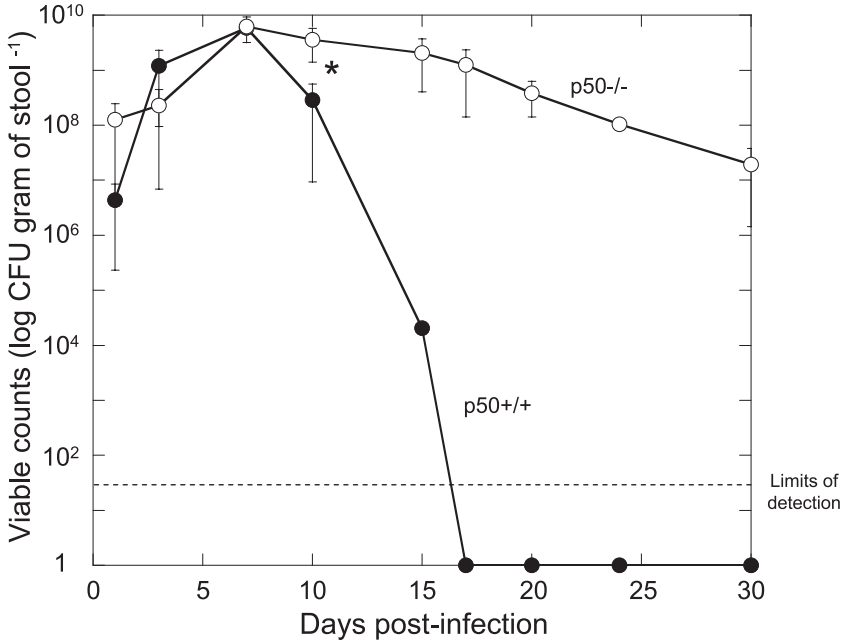

FIG. 1. Mice lacking the p50 subunit of NF-κB show prolonged shedding of bacteria in stools, suggesting a reduced ability to clear *C. rodentium* infection. In vivo colonization and clearance dynamics were monitored in $p50^{+/+}$ control (closed circles) and $p50^{-/-}$ (open circles) mice during *C. rodentium* infection by measuring bacterial viable counts recovered from stool. Mice lacking p50 shed significantly ($P < 0.05$) more bacteria than control mice from day 10 p.i. onward. The error bars indicate standard deviations.

nucleus and bind to the response elements of target promoters (16). Recently, Wang and colleagues demonstrated that NF-κB activity increased dramatically 12 days postinfection (p.i.) of Swiss-Webster mice with *C. rodentium* (30). Furthermore, they showed that NF-κB activation during *C. rodentium* infection predominantly involved p50/p65 heterodimer formation, but also p50/p50 homodimers.

Mice with targeted deletions of the immune system have proved extremely informative in relating particular arms of the immune response to immunity and pathology. Knockout of the p65 subunit of NF-κB is embryonic lethal in mice (3). In contrast, knockout of p50 has no effect on the growth of mice, and animals show few developmental abnormalities in the immune system. However, they do show deficiencies in immune response and are prone to infection (26).

Since *C. rodentium* infection results in upregulation of p65/p50 and p50/p50 NF-κB dimers (30), we have characterized the infection dynamics, immune response, and immune pathology of transgenic mice in which the p50 subunit of NF-κB has been knocked out ($p50^{-/-}$) during infection with *C. rodentium.* These studies were facilitated by the use of a bioluminescent derivative of *C. rodentium* (31) whose colonization and transmission dynamics can be followed, through its light emission, in a living mouse host (32).

MATERIALS AND METHODS

Bacterial strains and culture conditions. The bacterial strain used in this study was the bioluminescent *C. rodentium* derivative ICC180 (nalidixic acid and kanamycin resistant) (31). Bacteria were grown with shaking in Luria-Bertani (LB) medium at 37°C with antibiotics (kanamycin [100 μg ml^{-1}] or nalidixic acid [50 μg ml^{-1}]).

Mice. Female 6- to 8-week-old $p50^{-/-}$ (B6;129P-*Nfkb1*^{tm1Bal}/J [002849]) and $p50^{+/+}$ control (B6;129PF/J [100903]) mice were purchased from Jackson Laboratories (Bar Harbor, ME) and came from specific-pathogen-free stocks. All animals were housed in individually HEPA-filtered cages with sterile bedding and free access to sterilized food and water. Experiments were performed in accordance with the Animal Scientific Procedures Act (1986) and were approved by the local ethical review committee. Independent experiments were performed twice using four to six mice per group.

Oral infection of mice. Mice were orally inoculated using a gavage needle with 200 μl of overnight LB-grown bacterial suspension in phosphate-buffered saline (PBS) (~5×10^9 CFU) The number of viable bacteria used as an inoculum was determined by retrospective plating onto LB agar containing antibiotics. Stool samples were recovered aseptically at various time points after inoculation, and the number of viable bacteria per gram of stool was determined after homogenization at 0.1 g ml^{-1} in PBS and plating onto LB agar containing antibiotics. At selected time points p.i., blood was collected by cardiac puncture, and mice were sacrificed by cervical dislocation. Pieces of distal colon were collected and snap-frozen in liquid nitrogen before storage at −70°C prior to analysis.

In vivo bioluminescence imaging. Prior to being imaged, the abdominal region of each mouse was depilated to minimize any potential signal impedance by melanin within pigmented skin and fur. The bioluminescence (photons s^{-1} cm^{-2} sr^{-1}) from living infected animals was measured after gaseous anesthesia with isoflurane using the IVIS50 camera system (Xenogen). The sample shelf was set to position D (field of view, 15 cm). A photograph (reference image) was taken under low illumination prior to quantification of the photons emitted from ICC180 at a binning of 4 over 1 to 10 min using the software program Living Image (Xenogen) as an overlay on Igor (Wavemetrics, Seattle, WA). For anatomical localization, a pseudocolor image representing light intensity (blue, least intense, to red, most intense) was generated using the Living Image software and superimposed over the grayscale reference image. The bioluminescence within specific regions of individual mice was also quantified using the region-of-interest tool in the Living Image software program (given as photons s^{-1}).

Hematoxylin and eosin staining of frozen colonic sections. Frozen colonic tissues, embedded in OCT mounting medium (VWR BDH, Lutterworth, United Kingdom), were sectioned using a cryostat to a thickness of 5 μm. The sections were mounted on polysine slides (VWR BDH), air dried for 1 h, and then fixed in acetone for 20 min at room temperature before being dried for a minimum of 1 h. The sections were then stained according to standard protocols for hematoxylin and eosin staining. The colonic-crypt length (as an indication of hyperplasia) was measured using a graticule. Only well-oriented crypts were measured, and a minimum of 10 measurements were taken for each sample.

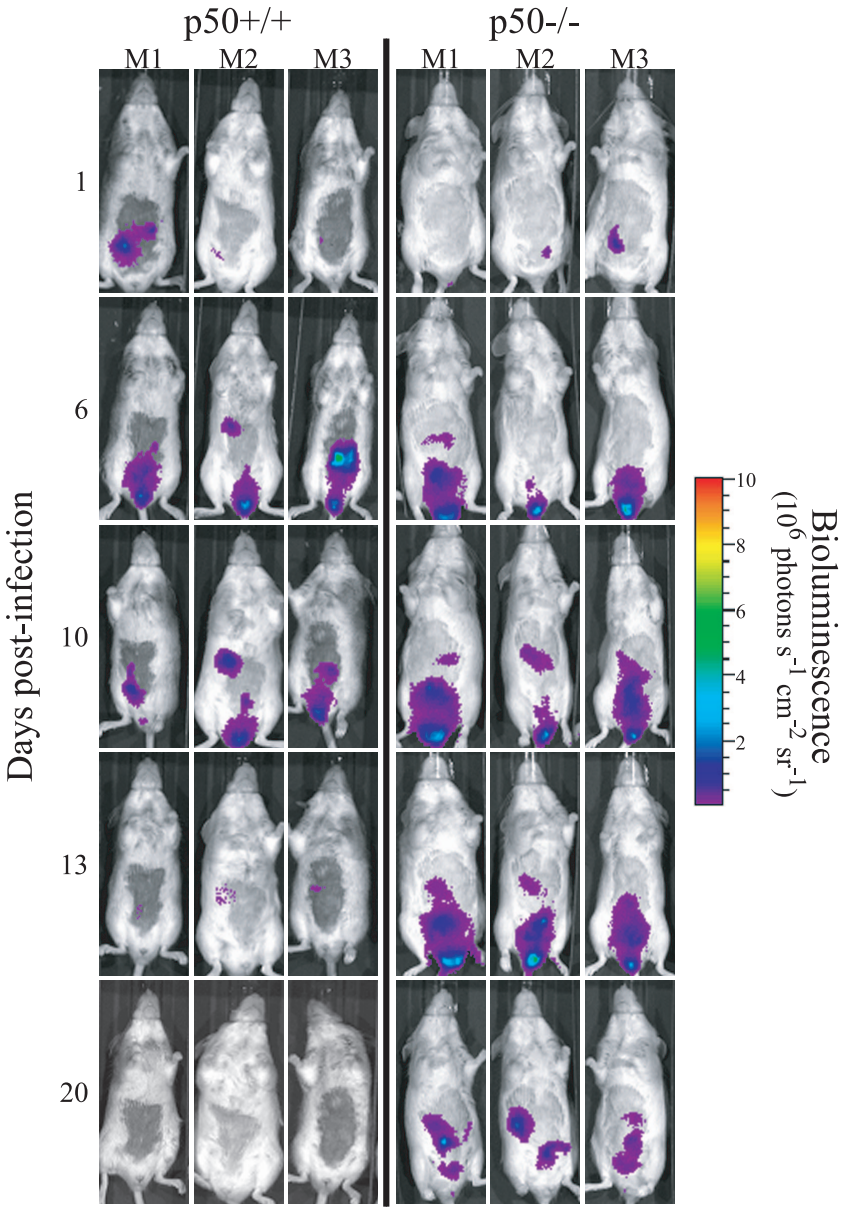

FIG. 2. Mice lacking the p50 subunit of NF-κB show prolonged carriage of *C. rodentium* in the abdominal region. In vivo colonization and clearance dynamics were monitored by BLI in $p50^{+/+}$ control mice (left) and $p50^{-/-}$ mice (right) during *C. rodentium* infection. The images were acquired using an IVIS50 system and are displayed as pseudocolor images of peak bioluminescence, with variations in color representing the light intensity at a given location. Red represents the most intense light emission, while blue corresponds to the weakest signal. The color bar indicates relative signal intensity. The mice were imaged at various time points p.i., with an integration time of 1 min. Three representative $p50^{+/+}$ control animals and three representative $p50^{-/-}$ animals are shown.

Immunohistochemistry. Cryostat sections of murine colon were rehydrated in Tris-buffered saline (TBS) for 5 min and then incubated with antibodies against CD3, CD4, CD8, F4/80, CD11c, NK1.1, or CD45R (Serotec, Oxford, United Kingdom) at a 1:10 to 1:100 dilution for 1 h. The sections were gently washed three times with TBS before the addition of biotinylated anti-rat or anti-hamster immunoglobulin G (IgG) (Serotec), as appropriate, at a dilution of 1:200 with 4% (vol/vol) normal murine serum for blocking (Sera Laboratories International, Horsted Keynes, United Kingdom) for 30 min. After the washing, a 1:200 dilution of 0.1% avidin-peroxidase (Sigma-Aldrich) was added for 30 min before further washing and the addition of diaminobenzadine substrate (Sigma-Aldrich) for 5 to 10 min. The reaction was stopped with excess TBS, and the sections were counterstained with hematoxylin and mounted as described above. A control slide using no primary antibody was also used to show endogenous peroxidase-containing cells. Stained cell populations were counted in five randomly selected fields per section, and the data were expressed as the number of T cells per 250 μm^2 of lamina propria.

ELISA. Proteins were extracted from approximately 15 mg of snap-frozen colonic tissue by homogenization in PBS plus protease inhibitor cocktail, sonicated three times in 10-s bursts, and then incubated in 1% Igepal lysis buffer for 20 min on ice with occasional vortexing. Supernatants were analyzed for cytokine levels using a Meso Scale Discovery (Gaithersburg, MA, USA) mouse proinflammatory 7-plex enzyme-linked immunosorbent assay (ELISA) kit (K11012B) and an SI6000 electrochemiluminescence plate reader, according to the manufacturer's instructions.

Determination of *C. rodentium*-specific antibody responses. An 18-h culture of *C. rodentium* was resuspended in PBS plus 1% bacterial protease inhibitor (Sigma-Aldrich Ltd., Dorset, United Kingdom) to an optical density at 600 nm (OD_{600}) of 1.0 and then heat killed at 60°C for 1 h. A 1:50 PBS dilution of this

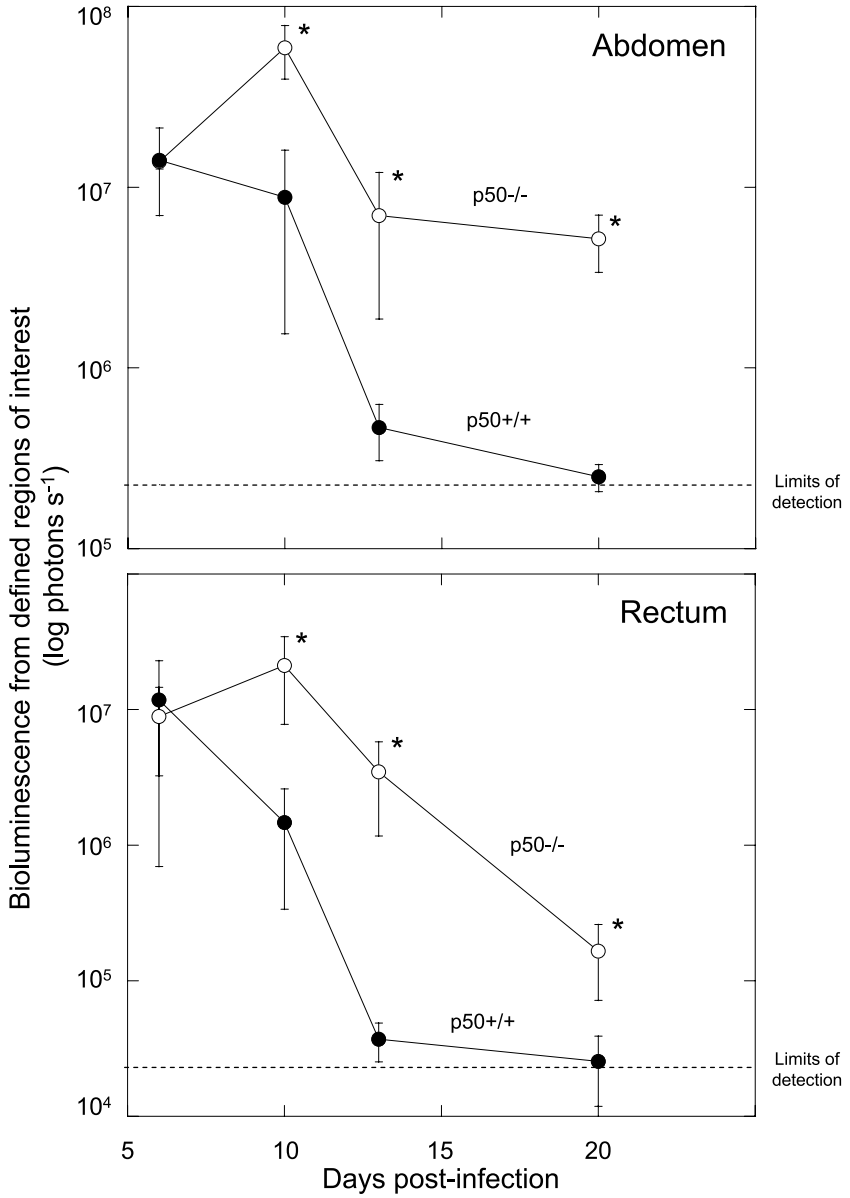

FIG. 3. Mice lacking the p50 subunit of NF-κB show prolonged carriage of *C. rodentium* in the abdominal region but clearance of the organism from the rectum. Shown is quantification of the bioluminescent signal originating from within specific regions of defined size (abdomen [top] and rectum [bottom]) in $p50^{+/+}$ mice (closed circles) and $p50^{-/-}$ mice (open circles) during *C. rodentium* infection. The values were obtained using the region-of-interest tool in the Living Image software program. The dotted lines represent the levels of background from uninfected animals. The error bars indicate standard deviations. *, statistically significant ($P < 0.05$) differences.

culture was added to ELISA plates (BD Biosciences, Oxford, United Kingdom) at 100 μl per well before incubation at 4°C overnight. The plates were washed three times with 200 μl per well PBS plus 0.05% Tween and then blocked for 1 h with 200 μl per well 1% bovine serum albumin in PBS blocking buffer. At selected time points postinoculation, blood was collected from the mice by cardiac puncture and centrifuged at 8,000 × g to separate red blood cells from serum. The *C. rodentium*-coated ELISA plates were washed as described previously, and then serum samples diluted 1:100 with PBS were added in duplicate wells (50 μl per well) and incubated at room temperature for 2 h. The plates were washed as before and then incubated at room temperature for 2 h with 100 μl per well 1:2,000 blocking buffer dilutions of rat anti-mouse IgG, IgG2b, IgG3, or IgM conjugated to alkaline phosphatase (AbD Serotec, Oxford, United Kingdom). After the plates were washed, antibodies were detected with 100 μl per well 1-mg/ml *p*-nitrophenylphosphate (Sigma-Aldrich Ltd., Dorset, United Kingdom) for 5 to 10 min before the reaction was stopped with 25 μl per well 3 N NaOH. Absorbance was determined using a VersaMax microplate reader with Softmax-PRO software (Molecular Devices, California) at 405 nm.

Statistics. Nonparametric tests between two groups were carried out using a two-tailed Mann-Whitney U test statistic with Bonferroni's correction for multiple comparisons. A P value of <0.05 was taken as significant in all cases. All tests were performed using SPSS statistical software (SPSS Inc., Ilinois), and Bonferroni's correction was applied manually.

RESULTS

Mice lacking the p50 subunit of NF-κB show a reduced ability to clear *C. rodentium* infection. In vivo colonization and clearance dynamics were monitored in $p50^{+/+}$ control and

$p50^{-/-}$ mice during infection with *C. rodentium* ICC180 by following viable counts recovered from stools (given as CFU per gram of stool) (Fig. 1) and using noninvasive bioluminescence imaging (BLI) (given as photons s^{-1} cm^{-2} sr^{-1}) (Fig. 2). In addition to information regarding localization, it is also possible to quantify the bioluminescence signal using Living Image software (Fig. 3) to give a measure of the pathogen burden in vivo (given as photons s^{-1}). Both shedding of *C. rodentium* in stool and BLI imaging from $p50^{+/+}$ control mice showed that these animals have an infection profile very similar to that of C57BL/6J mice reported previously (31, 32). In these mice, bioluminescence was localized as early as day 1 p.i. to a single focus within the abdominal region, which we had previously identified to be the cecal patch (31). Following adaptation within the cecum, both bioluminescence data and viable counts demonstrated that the challenge bacterial population colonized the distal colon and increased in number, reaching a plateau of ca. 6×10^9 CFU g of $stool^{-1}$ at day 8 p.i. (Fig. 1). At that time, the bioluminescent signal was localized throughout the abdominal region (corresponding to colonization of the cecum and colon) and rectum (Fig. 2). The mice began to clear the infection from day 10 p.i., which corresponded to a decrease in bioluminescence, until by day 13 p.i., a low signal was detectable (ca. 4×10^5 photons s^{-1}) that required a 10-min exposure to be visualized (Fig. 2). By day 17 p.i., all wild-type control mice had cleared the infection, with *C. rodentium* no longer detectable in the stool (Fig. 1). Similarly, $p50^{-/-}$ mice showed comparable early colonization dynamics, with the challenge bacterial population increasing in number and reaching a plateau at near-identical levels at day 8 p.i. (Fig. 1). However, in contrast to wild-type control animals, $p50^{-/-}$ mice were unable to clear the infection on the timescale examined. From day 10 p.i., levels of *C. rodentium* in $p50^{-/-}$ mice were significantly ($P < 0.05$) higher than in wild-type controls and, although beginning to fall, remained detectable by both BLI and viable counts in stool (ca. 10^7 CFU g of $stool^{-1}$ were still being shed at day 30 p.i.) (Fig. 1, 2, and 3). Indeed, the numbers of bacteria shed in stool remained high, although with much more variation between animals (range, ca. 10^4 to 10^7 CFU g of $stool^{-1}$), until at least day 42 (data not shown). Interestingly, while levels of *C. rodentium* stabilized within the abdominal region (ca. 10^6 photons s^{-1}) between days 13 and 20 p.i., light levels from within the region of the rectum and distal colon fell steadily (Fig. 3), suggesting some clearance from the rectum and/or distal colon. Importantly, there was no evidence of systemic spread of *C. rodentium* in $p50^{-/-}$ mice, with ICC180 undetectable in spleens or mesenteric lymph nodes (data not shown).

Mice lacking p50 develop significant prolonged colonic mucosal hyperplasia in response to infection with *C. rodentium*. A hallmark of *C. rodentium* infection is the development of colonic hyperplasia (measured by increased crypt length and weight). Interestingly, uninfected $p50^{-/-}$ mice had longer crypt lengths than uninfected $p50^{+/+}$ animals, evidence of spontaneous typhlocolitis, as previously described (9) (Fig. 4). However, there was a significant increase in crypt length in the $p50^{-/-}$ mice between day 0 and day 6 p.i., indicative of the rapid generation of a hyperplastic response to *C. rodentium* infection. Indeed, at day 6 p.i., hyperplasia was significantly greater in $p50^{-/-}$ mice than in infected controls and remained

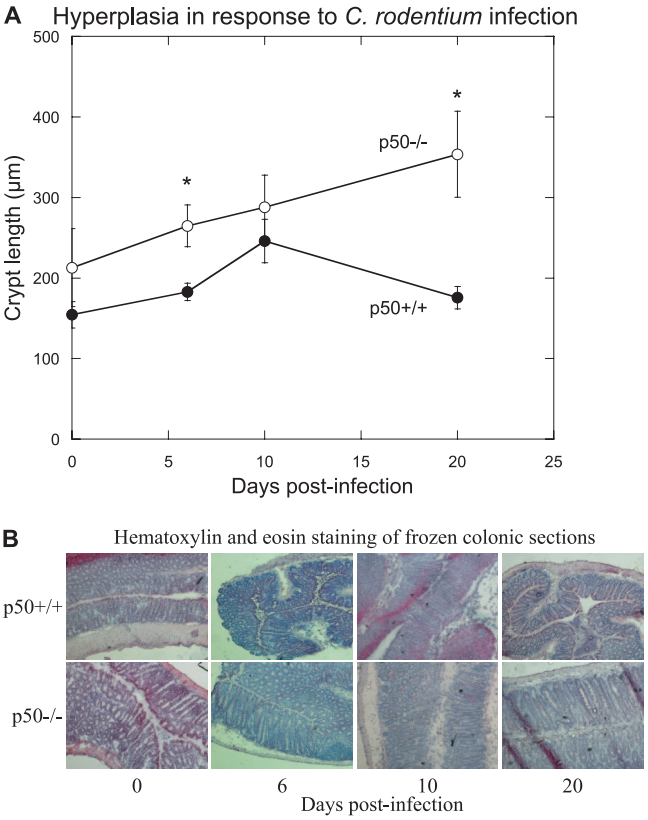

FIG. 4. Mice lacking p50 develop significant prolonged colonic mucosal hyperplasia in response to infection with *C. rodentium*. (A) Colonic hyperplasia was assessed during *C. rodentium* infection of $p50^{+/+}$ mice (closed circles) and $p50^{-/-}$ mice (open circles) by measuring the crypt lengths of frozen colonic sections after hematoxylin and eosin staining. The error bars indicate standard deviations. *, statistically significant ($P < 0.05$) differences. (B) Hematoxylin and eosin staining of frozen colonic sections taken at various time points p.i. for wild-type control (top) and $p50^{-/-}$ (bottom) animals.

at a high level to day 20 p.i. (Fig. 4), mirroring the high bacterial burdens seen in these animals (Fig. 1). In contrast, control mice developed peak hyperplasia by day 10 p.i., with crypt length returning to near-normal levels by day 20, once the infection was resolved (Fig. 4). By day 42 p.i., those $p50^{-/-}$ mice with very high pathogen burdens (ca. 10^7 CFU g of $stool^{-1}$) still demonstrated considerable levels of hyperplasia (crypt lengths of >300 μm), indicating a severe infection with increased damage to the gut epithelium (data not shown). However, at that time point, the crypt lengths of the $p50^{-/-}$ mice with lower pathogen burdens (ca. 10^5 CFU g of $stool^{-1}$) appeared to be returning to uninfected levels (crypt lengths, ca. 200 μm) (data not shown), suggesting that a critical bacterial burden is required for maintenance of hyperplasia.

Mice lacking p50 show delayed and reduced immune cell infiltration into colonic tissue during *C. rodentium* infection. Frozen sections of colon were stained with antibodies against CD3, CD4, CD8, F4/80 (as a marker for macrophages), CD11c (as a marker for dendritic cells), NK1.1 (as a marker for NK cells), or CD45R (also known as B220, as a marker for B cells). Wild-type control mice infected with *C. rodentium* showed a characteristic immune cell influx into infected colonic tissue,

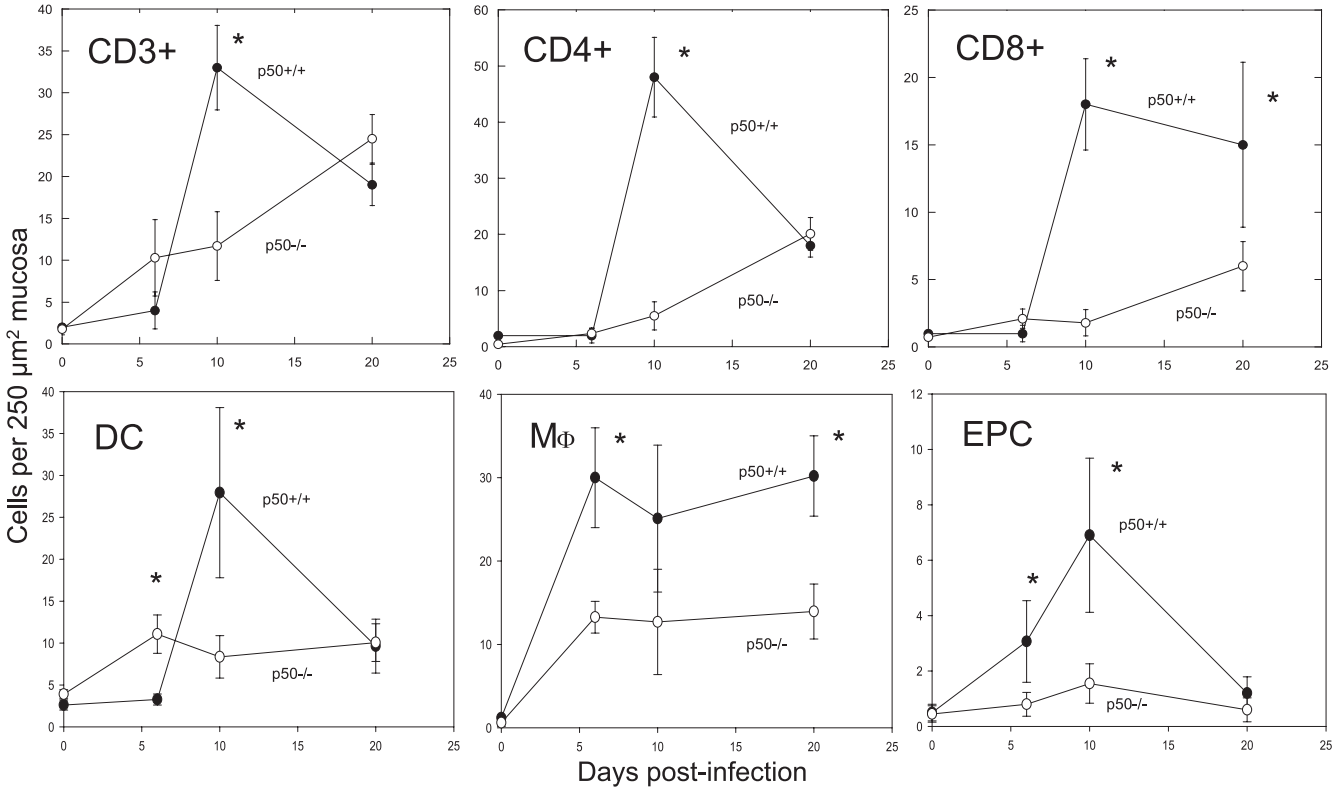

FIG. 5. Mice lacking p50 show delayed and reduced immune cell infiltration into colonic tissue during *C. rodentium* infection. Immune cell infiltrates were measured during *C. rodentium* infection of $p50^{+/+}$ mice (closed circles) and $p50^{-/-}$ mice (open circles) using frozen sections of murine colon incubated with antibodies against CD3 (top left), CD4 (top middle), CD8 (top right), CD11c as a marker for dendritic cells [DC] (bottom left), and F4/80 as a marker for macrophages [Mϕ] (bottom middle). A control slide using no primary antibody was also used to show endogenous peroxidase-containing cells (EPC) (most commonly neutrophils) (bottom right). The error bars indicate standard deviations. *, statistically significant ($P < 0.05$) differences.

with levels of $CD3^+$, $CD4^+$, $CD8^+$, dendritic, and endogenously peroxidase-stained cells (most commonly neutrophils) (given as cells 250 μm mucosa^{-2}) peaking at day 10 p.i. (Fig. 5 and 6). The numbers of macrophages peaked earlier, at day 6 p.i., and remained high throughout (Fig. 5). The numbers of $CD3^+$, $CD4^+$, and dendritic cells and neutrophils began subsiding by day 20 p.i. (Fig. 5) as the bacteria were cleared from the gut. In contrast, the $p50^{-/-}$ mice failed to show the rapid infiltrative response of the $p50^{+/+}$ mice, suggesting that immune cell proliferation or recruitment to infected mucosal tissues was defective. Instead, $p50^{-/-}$ mice showed a gradual influx of immune cells, with cell counts at the normal peak of infection (day 10) significantly ($P < 0.05$) reduced compared to infected controls despite an increased bacterial burden (Fig. 5 and 6). Tissue harvested from infected $p50^{-/-}$ mice at days 36 and 42 p.i. showed a continued gradual influx in $CD4^+$ T cells and only a slight decrease in $CD3^+$ and $CD8^+$ cells (data not shown). Staining for B cells and NK cells revealed no influx into infected tissue of either $p50^{-/-}$ or $p50^{+/+}$ mice (data not shown).

Mice lacking p50 still develop significant cytokine responses in colonic tissue during *C. rodentium* infection. Tissues collected at days 0, 6, 10, and 20 p.i. with *C. rodentium* were assayed for the anti-inflammatory cytokine interleukin 10 (IL-10) and the proinflammatory cytokines gamma interferon (IFN-γ), tumor necrosis factor alpha (TNF-α), IL-1β, chemokine (CXC motif) ligand 1 (KC), and IL-6 by ELISA (Fig. 7) and confirmed by quantification of mRNA transcripts (data not shown). As expected, levels of IFN-γ and TNF-α steadily increased in infected $p50^{+/+}$ mice, peaking at day 10 p.i. and decreasing to uninfected levels by day 20 p.i. Similarly, levels of IFN-γ and TNF-α also increased in $p50^{-/-}$ mice. However, by day 20 p.i., the levels of these cytokines were significantly ($P < 0.05$) higher than in $p50^{+/+}$ mice, correlating with the lack of clearance of *C. rodentium* infection. Measurement of the cytokines IL-1β and IL-6 during the first 10 days p.i. showed that the levels remained relatively low, with no difference between $p50^{-/-}$ and $p50^{+/+}$ mice. In contrast, both IL-1β and IL-6 levels were significantly ($P < 0.05$) higher in $p50^{-/-}$ mice at day 20 p.i. Levels of KC steadily increased in infected $p50^{+/+}$ mice, peaking at day 10 p.i. and decreasing to uninfected levels by day 20 p.i. In contrast, KC levels in $p50^{-/-}$ mice were significantly ($P < 0.05$) higher, both in uninfected tissues and during infection, and remained high throughout. There were no significant changes in the levels of the anti-inflammatory cytokine IL-10 during *C. rodentium* infection for either the $p50^{-/-}$ or $p50^{+/+}$ animals.

Mice lacking p50 exhibit no major defects in antibody response to *C. rodentium*. Since antibody responses have been implicated in the resolution of *C. rodentium* infection (5), the

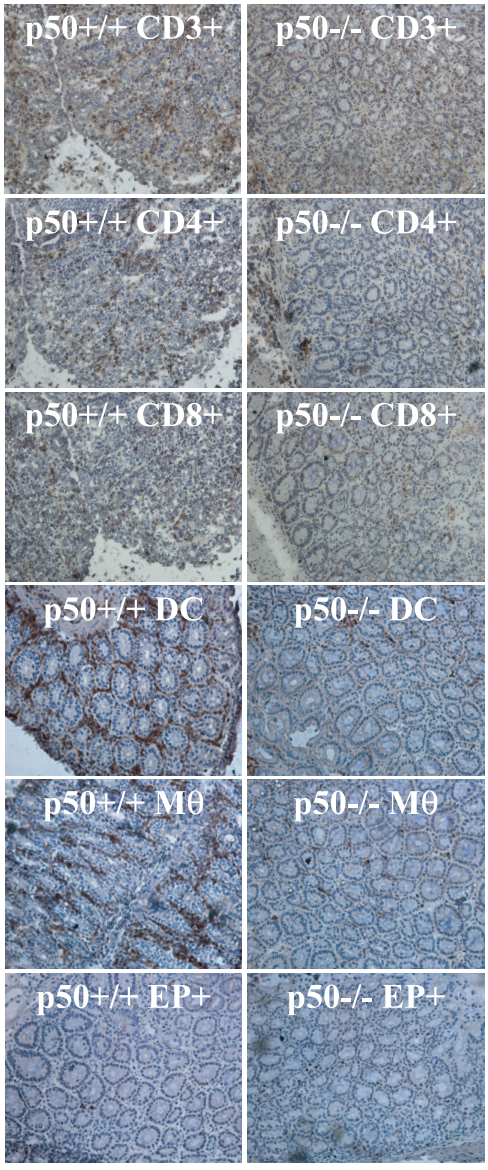

FIG. 6. Mice lacking p50 show reduced immune cell infiltration into colonic tissue at the peak of *C. rodentium* infection. Frozen sections of murine colon show that immune cell infiltrates peaked in wild-type control mice (left) at day 10 p.i., whereas $p50^{-/-}$ mice (right) show delayed immune cell infiltration: $CD3^+$ cells (top), $CD4^+$ cells, $CD8^+$ cells, dendritic cells (DC), macrophages (Mϕ), and endogenous peroxidase-containing cells (neutrophils) (EP+). (Magnification, ×20).

C. rodentium-specific antibody responses of $p50^{-/-}$ mice were analyzed by ELISA. Contrary to previously published reports (26), $p50^{-/-}$ mice did not exhibit defects in immunogen-specific antibody responses, although considerable variation was seen between individual $p50^{-/-}$ mice (Fig. 8). In addition, we did not observe defects in isotype switching, with considerable IgG2b and IgG3 responses by day 20 in $p50^{-/-}$ mice. Total IgG and IgG2b responses were significantly delayed, with reduced amounts at days 6 and 10 relative to controls. However, by day 20, there were no significant differences between all IgG isotypes. In addition, the IgM response in $p50^{-/-}$ animals was significantly higher than that of wild-type controls by day 20, possibly as a result of the large bacterial burden at the gut mucosal surface. Even with these antibody responses that were similar to or greater than those of the control, *C. rodentium* was still not cleared from the gastrointestinal tract.

DISCUSSION

Whereas the adaptive immune responses to A/E pathogens have been well investigated, the role of the innate immune response is less well understood. The transcription factor NF-κB, most commonly a heterodimer composed of p50 and p65 subunits, is of critical importance in the activation and regulation of the immune response (16). It is ubiquitously expressed in most cell types and regulates a variety of genes responsible for immune function and inflammation (23, 26). While knockout of the p65 subunit of NF-κB is embryonic lethal in mice (3), knockout of p50 has no effect on growth, and $p50^{-/-}$ animals show few developmental abnormalities in the immune system (26). The effect of NF-κB knockout on the infection kinetics of an A/E lesion-forming pathogen is particularly interesting, since recent evidence has suggested A/E pathogens may actively inhibit NF-κB activation, indicating its importance to the host immune response (14). The present study was initiated to determine the role of the p50 subunit of NF-κB in the immune response to *C. rodentium*.

Despite previous data showing that p50 knockout results in B-cell proliferation, antibody production, and antibody isotype-switching defects (26, 29), we observed substantial IgG and IgM responses in $p50^{-/-}$ animals infected with *C. rodentium.* These findings are supported by the work of Snapper et al., who indicated that synergistic signaling can overcome dependence on signaling via p50 (29). For example, membrane-bound immunoglobulin signaling in combination with lipopolysaccharide signaling can restore $p50^{-/-}$ B-cell proliferation to near-normal levels (29).

In our investigation, $p50^{-/-}$ mice were unable to resolve infection with *C. rodentium* within the time frame studied and showed significantly greater pathology than infected wild-type controls. Our observation that $p50^{-/-}$ animals were able to mount a substantial IgG response and yet were unable to resolve infection is somewhat surprising, since previous research had indicated that protective immunity was mediated by IgG (5). In previous work, intravenous administration of serum IgG and IgM successfully circumvented the severe and often lethal pathology seen in $CD4^{-/-}$ mice and led to clearance of the bacteria from the gut. In our system, however, a reduction in CD4 responses coupled with substantial (although delayed) antibody responses did not lead to clearance, indicating there is more to protective immunity than IgG alone. In addition, $CD4^{-/-}$ mice showed significant mortality during *C. rodentium* infection (6), whereas $p50^{-/-}$ mice with a profound reduction in $CD4^+$ T-cell recruitment into infected tissues did not. $CD4^{-/-}$ mouse mortality was attributed to polymicrobial sepsis, probably as a result of deficiency in IgG responses. In $p50^{-/-}$ animals, on the other hand, IgG responses were not affected, and thus systemic immunity to *C. rodentium* was not reduced. Indeed, spleens and mesenteric lymph nodes from $p50^{-/-}$ mice were negative for *C. rodentium*, indicating sys-

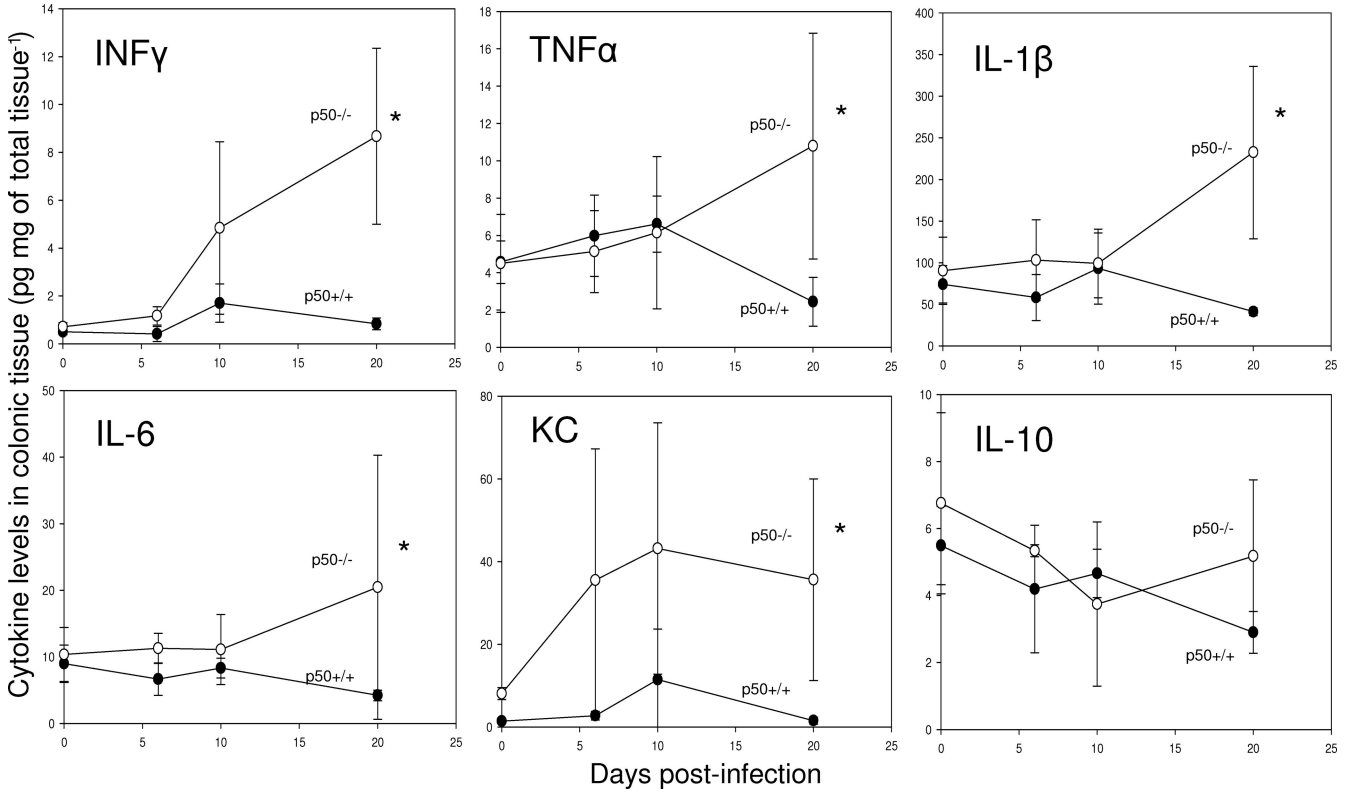

FIG. 7. Mice lacking p50 develop significant cytokine responses in colonic tissue during *C. rodentium* infection. Cytokine levels were measured during *C. rodentium* infection of $p50^{+/+}$ mice (closed circles) and $p50^{-/-}$ mice (open circles) using frozen sections of murine colon. The error bars indicate standard deviations. *, statistically significant ($P < 0.05$) differences.

temic immunity was still in place, despite the lack of immune cell recruitment.

The hypothesis that early circulating antibody might control the pathogen burden during *C. rodentium* infection (6) is supported by our data, since $p50^{-/-}$ mice showed delayed antibody responses and increased bacterial burdens. Mice deficient in p50 have previously been shown to lack marginal-zone B cells at peripheral lymphoid sites that in normal mice rapidly differentiate into antibody-secreting plasma B cells (26). This may explain the delay in antibody responses observed in this study and may contribute to the increased pathogen burden experienced by these animals.

Although there is clear evidence that NF-κB plays a key role in the expression of proinflammatory cytokines in response to A/E pathogens (11, 25), compensatory effects by other NF-κB family members and alternative signaling pathways (such as transcription factor activator protein [AP-1]) suggest that p50 is not essential in activating these cytokine responses. Indeed, our results indicate that a lack of p50 does not prevent the expression of cytokines, including IL-1β, IFN-γ, TNF-α, IL-6, and KC. The elevated cytokine secretion by infected $p50^{-/-}$ mice has been observed for a variety of pathogens (1, 4, 9, 10), in association with a failure to clear infection, and thus may be a deliberate attempt by the host to boost immune responses and resolve infection. Increased cytokine levels may also be a side effect of the continued and increased pathogen burden in these animals. Our data showed that the cytokine IL-10 was unaffected in $p50^{-/-}$ animals, and thus, the high levels of cytokines observed in this system are not likely to be due to loss of inhibition by this anti-inflammatory cytokine. Further studies are required to identify the possible inhibitory mechanisms of p50 and to separate the effects of high bacterial burden from the effects of the lack of p50.

As reported for infection of $p50^{-/-}$ mice with the parasite *Leishmania major* (2), and despite heightened cytokine levels at the peak of infection (day 10), we observed a profound recruitment defect in $CD4^+$ T-cell infiltrates into infected $p50^{-/-}$ colonic tissue. In addition, we also identified a significant reduction in $CD3^+$ and $CD8^+$ T cells, macrophages, neutrophils, and dendritic cells in infected tissues, indicating that in this system, mice lacking p50 fail to mobilize the appropriate immune response, leading to a failure to resolve infection.

Despite the observed low level of $CD4^+$ T cells, we did not see a reduction in IFN-γ in infected tissue. Staining for NK cells (a second significant producer of IFN-γ) showed no influx in wild-type or $p50^{-/-}$ infected animals, indicating that these cells were not the source of IFN-γ. The apparent paradox presented by high levels of IFN-γ but small numbers of cells capable of producing this cytokine can be explained if the few T cells present in $p50^{-/-}$ infected tissue are being stimulated to produce large amounts of cytokine, a hypothesis that requires further investigation.

Although $p50^{-/-}$ animals show no developmental or growth defects, some evidence suggests they may be prone to spontaneous colitis, particularly in the cecum (9). In our experiments,

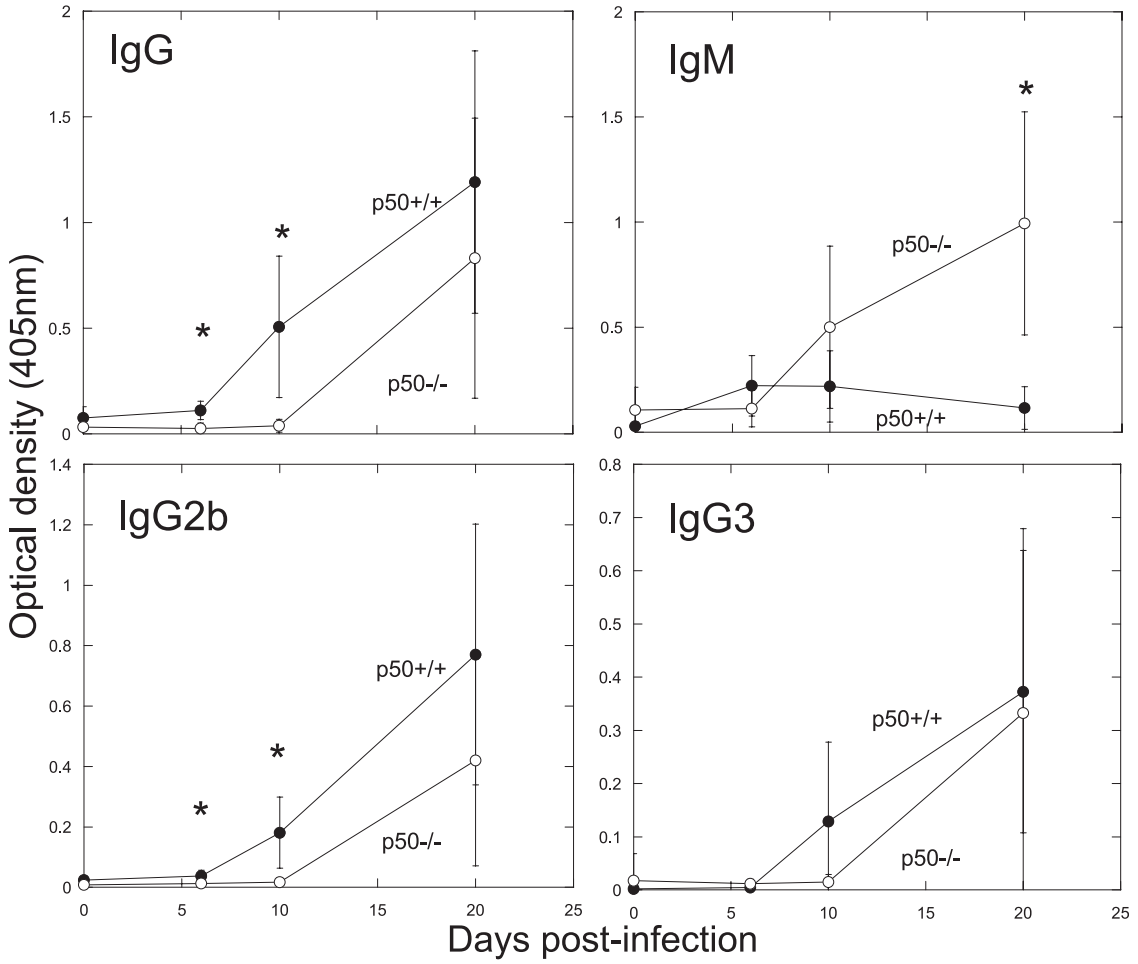

FIG. 8. Mice lacking p50 exhibit a delayed antibody response to *C. rodentium.* Shown are total IgG (top left), IgM (top right), IgG2b (bottom left), and IgG3 (bottom right) antibody responses (as measured by ELISA) in colonic tissue of $p50^{+/+}$ (closed circles) and $p50^{-/-}$ (open circles) mice during *C. rodentium* infection. The error bars indicate standard deviations. *, statistically significant differences.

young animals were used to minimize this possibly confounding spontaneous colitis, but some evidence of colonic hyperplasia was seen at day 0 in $p50^{-/-}$ animals. However, since a significant difference in hyperplasia was seen between day 0 and day 10 in infected $p50^{-/-}$ animals, we can be confident that infectious colitis was occurring over and above any possible spontaneous background colitis. It is interesting that even in the absence of an inflammatory infiltrate, $p50^{-/-}$ mice still showed a hyperplastic response. Previous research had also shown hyperplastic responses in the absence of the proinflammatory cytokines IFN-γ and TNF-α (27), thus indicating that hyperplasia may be an innate response of enteric epithelial cells. It would be interesting to investigate this hypothesis further.

Recently, Toll-like receptor signaling through the adaptor molecule MyD88 has been reported to be essential for survival and optimal immunity following infection with *C. rodentium* (15). MyD88 is one of many adaptor molecules that can activate the transcription factor NF-κB. Hence, it is possible that a knockout of MyD88 may reduce the activity of NF-κB, resulting in similar pathological outcomes when $MyD88^{-/-}$ and $p50^{-/-}$ animals are infected with *C. rodentium*.

Infection of $MyD88^{-/-}$ mice with *C. rodentium* resulted in severe colitis, including localized intramural colonic bleeding and gangrenous mucosal necrosis associated with large colonies of bacteria, and a mortality rate of 100% by day 13 p.i. (15). Although *C. rodentium*-infected $p50^{-/-}$ animals displayed a more severe colitis than wild-type controls, they did not show the same mucosal pathology as $MyD88^{-/-}$ animals and did not show an increase in mortality. Interestingly, the main characteristic of *C. rodentium* infection, a hyperplastic response by epithelial cells, was not seen in $MyD88^{-/-}$ animals, while $p50^{-/-}$ mice showed considerable hyperplasia compared to infected wild-type control animals. This indicates that hyperplastic responses, indicative of wound repair by epithelial cells, are $MyD88^{-/-}$ but not NF-κB dependent. A lack of wound repair may explain the increased mucosal pathology in $MyD88^{-/-}$ compared to $p50^{-/-}$ mice.

Similar to our data from $p50^{-/-}$ mice, adaptive immune responses to infection were observed in $MyD88^{-/-}$ mice, including a protective antibody response (15). In agreement with our own results, Lebeis et al. found this antibody response insufficient for clearance (15), suggesting that other arms of the immune response are important, particularly at mucosal sites.

This is supported by data showing that reconstituting antibody responses in MyD88$^{-/-}$ mice results in eventual clearance, but with delayed infection kinetics (15).

It was suggested that reduced wound repair or neutrophil responses might explain the lack of resolution of infection in Myd88$^{-/-}$ mice (15). In p50$^{-/-}$ mice, we did not see a reduction in wound repair (evidenced by the considerable hyperplastic response) but did observe significantly reduced neutrophil responses despite very high levels of the cytokine KC, a neutrophil chemoattractant. This reduction in neutrophils may explain the lack of resolution seen in p50$^{-/-}$ animals. In addition, we suggest that a delay in adaptive immune responses (both antibody and T-cell responses) seen in infected p50$^{-/-}$ mice leads to considerable bacterial burdens that are beyond the capabilities of later responses to control and clear. It is possible that defects or delays in early innate immune responses may also contribute to this increase in bacterial burden, since innate immune cells are known to control the colonization level and prevent bacteremia by maintaining the epithelial barrier. Indeed Lebeis et al. observed a delay in chemokine production early in infection of Myd88$^{-/-}$ animals, resulting in a delay in innate immune responses, particularly neutrophil migration (15). It would be interesting to investigate other early innate immune responses in both MyD88$^{-/-}$ and p50$^{-/-}$ animals to assess their impacts on later resolution of infection.

This work shows for the first time the importance of p50 in the immune response to a noninvasive enteric A/E lesion pathogen. The failure to resolve infection and increased pathology seem to be common features of p50$^{-/-}$ mice and have been observed in previous studies of both intracellular and extracellular pathogens, as well as pathogens that induce both TH1 and TH2 immune responses (1, 2, 26). The similarity in outcomes between such varying infections and our results using a noninvasive enteric pathogen suggest that the p50 subunit of NF-κB is central to a common process that occurs in the majority of immune responses. Although p50 is known to be proinflammatory early in the response to infection, it also has inhibitory functions that appear to prevent extended inflammatory responses and immune-mediated host damage (1, 26). The loss of these inhibitory functions in p50$^{-/-}$ mice would explain the apparent failure to control infection-induced inflammation, resulting in the increased pathology observed by us and others. Indeed the high proinflammatory cytokine and antibody responses observed in p50$^{-/-}$ animals would indicate such a loss of inhibition, although this may also be due, at least in part, to the prolonged and high pathogen burden seen in p50$^{-/-}$ mice infected with *C. rodentium*.

In conclusion, we have demonstrated that non-p50-dependent defenses are not sufficient to control infection progression with a noninvasive enteric pathogen, and hence, the p50 subunit of NF-κB is essential for defense against *C. rodentium*.

ACKNOWLEDGMENT

This work was supported by the Wellcome Trust.

REFERENCES

1. **Artis, D., S. Shapira, N. Mason, K. M. Speirs, M. Goldschmidt, J. Caamano, H. C. Liou, C. A. Hunter, and P. Scott.** 2002. Differential requirement for NF-kappa B family members in control of helminth infection and intestinal inflammation. J. Immunol. **169:**4481–4487.
2. **Artis, D., K. Speirs, K. Joyce, M. Goldschmidt, J. Caamano, C. A. Hunter, and P. Scott.** 2003. NF-kappa B1 is required for optimal CD4$^+$ Th1 cell development and resistance to *Leishmania major*. J. Immunol. **170:**1995–2003.
3. **Beg, A. A., W. C. Sha, R. T. Bronson, S. Ghosh, and D. Baltimore.** 1995. Embryonic lethality and liver degeneration in mice lacking the RelA component of NF-kappa B. Nature **376:**167–170.
4. **Bohuslav, J., V. V. Kravchenko, G. C. Parry, J. H. Erlich, S. Gerondakis, N. Mackman, and R. J. Ulevitch.** 1998. Regulation of an essential innate immune response by the p50 subunit of NF-κB. J. Clin. Investig. **102:**1645–1652.
5. **Bry, L., and M. B. Brenner.** 2004. Critical role of T cell-dependent serum antibody, but not the gut-associated lymphoid tissue, for surviving acute mucosal infection with *Citrobacter rodentium*, an attaching and effacing pathogen. J. Immunol. **172:**433–441.
6. **Bry, L., M. Brigl, and M. B. Brenner.** 2006. CD4$^+$-T-cell effector functions and costimulatory requirements essential for surviving mucosal infection with *Citrobacter rodentium*. Infect. Immun. **74:**673–681.
7. **Deng, W., J. L. Puente, S. Gruenheid, Y. Li, B. A. Vallance, A. Vazquez, J. Barba, J. A. Ibarra, P. O'Donnell, P. Metalnikov, K. Ashman, S. Lee, D. Goode, T. Pawson, and B. B. Finlay.** 2004. Dissecting virulence: systematic and functional analyses of a pathogenicity island. Proc. Natl. Acad. Sci. USA **101:**3597–3602.
8. **Deng, W., B. A. Vallance, Y. Li, J. L. Puente, and B. B. Finlay.** 2003. *Citrobacter rodentium* translocated intimin receptor (Tir) is an essential virulence factor needed for actin condensation, intestinal colonization and colonic hyperplasia in mice. Mol. Microbiol. **48:**95–115.
9. **Erdman, S., J. G. Fox, C. A. Dangler, D. Feldman, and B. H. Horwitz.** 2001. Typhlocolitis in NF-kappa B-deficient mice. J. Immunol. **166:**1443–1447.
10. **Gadjeva, M., M. F. Tomczak, M. Zhang, Y. Y. Wang, K. Dull, A. B. Rogers, S. E. Erdman, J. G. Fox, M. Carroll, and B. H. Horwitz.** 2004. A role for NF-kappa B subunits p50 and p65 in the inhibition of lipopolysaccharide-induced shock. J. Immunol. **173:**5786–5793.
11. **Gobert, A. P., K. T. Wilson, and C. Martin.** 2005. Cellular responses to attaching and effacing bacteria: activation and implication of the innate immune system. Arch. Immunol. Ther. Exp. **53:**234–244.
12. **Higgins, L. M., G. Frankel, G. Douce, G. Dougan, and T. T. MacDonald.** 1999. *Citrobacter rodentium* infection in mice elicits a mucosal Th1 cytokine response and lesions similar to those in murine inflammatory bowel disease. Infect. Immun. **67:**3031–3039.
13. **Kaper, J. B., J. P. Nataro, and H. L. Mobley.** 2004. Pathogenic *Escherichia coli*. Nat. Rev. Microbiol. **2:**123–140.
14. **Klumpp, D. J., A. C. Weiser, S. Sengupta, S. G. Forrestal, R. A. Batler, and A. J. Schaeffer.** 2001. Uropathogenic *Escherichia coli* potentiates type 1 pilus-induced apoptosis by suppressing NF-κB. Infect. Immun. **69:**6689–6695.
15. **Lebeis, S. L., B. Bommarius, C. A. Parkos, M. A. Sherman, and D. Kalman.** 2007. TLR signaling mediated by MyD88 is required for a protective innate immune response by neutrophils to *Citrobacter rodentium*. J. Immunol. **179:**566–577.
16. **Li, Q., and I. M. Verma.** 2002. NF-κB regulation in the immune system. Nat. Rev. Immunol. **2:**725–734.
17. **Liou, H. C., and C. Y. Hsia.** 2003. Distinctions between c-Rel and other NF-κB proteins in immunity and disease. Bioessays **25:**767–780.
18. **Ma, C., M. E. Wickham, J. A. Guttman, W. Deng, J. Walker, K. L. Madsen, K. Jacobson, W. A. Vogl, B. B. Finlay, and B. A. Vallance.** 2006. *Citrobacter rodentium* infection causes both mitochondrial dysfunction and intestinal epithelial barrier disruption in vivo: role of mitochondrial associated protein (Map). Cell Microbiol. **8:**1669–1686.
19. **Maaser, C., M. P. Housley, M. Iimura, J. R. Smith, B. A. Vallance, B. B. Finlay, J. R. Schreiber, N. M. Varki, M. F. Kagnoff, and L. Eckmann.** 2004. Clearance of *Citrobacter rodentium* requires B cells but not secretory immunoglobulin A (IgA) or IgM antibodies. Infect. Immun. **72:**3315–3324.
20. **Monteleone, G., J. Mann, I. Monteleone, P. Vavassori, R. Bremner, M. Fantini, G. Del Vecchio Blanco, R. Tersigni, L. Alessandroni, D. Mann, F. Pallone, and T. T. MacDonald.** 2004. A failure of transforming growth factor-β1 negative regulation maintains sustained NF-κB activation in gut inflammation. J. Biol. Chem. **279:**3925–3932.
21. **Mundy, R., F. Girard, A. J. FitzGerald, and G. Frankel.** 2006. Comparison of colonization dynamics and pathology of mice infected with enteropathogenic *Escherichia coli*, enterohaemorrhagic *E. coli* and *Citrobacter rodentium*. FEMS Microbiol. Lett. **265:**126–132.
22. **Mundy, R., T. T. MacDonald, G. Dougan, G. Frankel, and S. Wiles.** 2005. *Citrobacter rodentium* of mice and man. Cell Microbiol. **7:**1697–1706.
23. **Neurath, M. F., C. Becker, and K. Barbulescu.** 1998. Role of NF-κB in immune and inflammatory responses in the gut. Gut **43:**856–860.
24. **Neurath, M. F., S. Pettersson, K. H. Meyer zum Buschenfelde, and W. Strober.** 1996. Local administration of antisense phosphorothioate oligonucleotides to the p65 subunit of NF-kappa B abrogates established experimental colitis in mice. Nat. Med. **2:**998–1004.
25. **Savkovic, S. D., A. Koutsouris, and G. Hecht.** 1997. Activation of NF-κB in

intestinal epithelial cells by enteropathogenic *Escherichia coli*. Am. J. Physiol. **273:**C1160–C1167.
26. **Sha, W. C., H. C. Liou, E. I. Tuomanen, and D. Baltimore.** 1995. Targeted disruption of the p50 subunit of NF-kappa B leads to multifocal defects in immune responses. Cell **80:**321–330.
27. **Simmons, C. P., N. S. Goncalves, M. Ghaem-Maghami, M. Bajaj-Elliott, S. Clare, B. Neves, G. Frankel, G. Dougan, and T. T. MacDonald.** 2002. Impaired resistance and enhanced pathology during infection with a noninvasive, attaching-effacing enteric bacterial pathogen, *Citrobacter rodentium*, in mice lacking IL-12 or IFN-gamma. J. Immunol. **168:**1804–1812.
28. **Simpson, N., R. Shaw, V. F. Crepin, R. Mundy, A. J. FitzGerald, N. Cummings, A. Straatman-Iwanowska, I. Connerton, S. Knutton, and G. Frankel.** 2006. The enteropathogenic *Escherichia coli* type III secretion system effector Map binds EBP50/NHERF1: implication for cell signalling and diarrhoea. Mol. Microbiol. **60:**349–363.
29. **Snapper, C. M., P. Zelazowski, F. R. Rosas, M. R. Kehry, M. Tian, D. Baltimore, and W. C. Sha.** 1996. B cells from p50/NF-kappa B knockout mice have selective defects in proliferation, differentiation, germ-line CH transcription, and Ig class switching. J. Immunol. **156:**183–191.
30. **Wang, Y., G. S. Xiang, F. Kourouma, and S. Umar.** 2006. *Citrobacter rodentium*-induced NF-κB activation in hyperproliferating colonic epithelia: role of p65 (Ser536) phosphorylation. Br. J. Pharmacol. **148:**814–824.
31. **Wiles, S., S. Clare, J. Harker, A. Huett, D. Young, G. Dougan, and G. Frankel.** 2004. Organ specificity, colonization and clearance dynamics in vivo following oral challenges with the murine pathogen *Citrobacter rodentium*. Cell Microbiol. **6:**963–972.
32. **Wiles, S., K. M. Pickard, K. Peng, T. T. MacDonald, and G. Frankel.** 2006. In vivo bioluminescence imaging of the murine pathogen *Citrobacter rodentium*. Infect. Immun. **74:**5391–5396.

Editor: A. Camilli